сообщения
объединенного
института
ядерных
исследований
дубна

E2-94-126

Kh.El-Waged[1], V.V.Uzhinskii*

REGGEON THEORY INSPIRED MODEL OF NUCLEAR DESTRUCTION IN HIGH ENERGY NUCLEUS-NUCLEUS INTERACTIONS

[1]On leave from Physics Department of Benha University, Egypt
*E-mail: UZHIN@LCTA9.JINR.DUBNA.SU

1994

1 INTRODUCTION

In the simplest approach the nucleon can be represented as a core surrounded by a cloud of virtual mesons. At low energies when the interaction time is greater than the mean life time of virtual meson $\tau \simeq 1/m_\pi$ many virtual mesons take part in the interaction and the nucleon looks like structureless system. At high energies τ is increased by the Lorentz-factor of incident hadron and the number of virtual mesons does not change during the interaction, the nucleons behave as quasi-nuclear structure. This structure can manifest itself in hadron-nucleus and nucleus-nucleus interactions. In the course of hadron-nucleus collisions different virtual mesons of projectile hadron can interact with different intranuclear nucleons. So the collisions cannot be represented as a set of simultaneously binary collisions of incident and produced hadrons with intranuclear nucleons. The picture of collective interaction becomes more adequate. Some arguments in favor of it were given in Ref. [1], where the problem of description of secondary particle cascading into the nucleus was considered in the framework of Reggeon theory.

In the reggeon theory the calculations of amplitudes and cross sections of cascade interactions require consideration of enhanced graphs. The simplest graphs were taken into account in papers [2, 3]. In Refs. [4, 5] an effective calculating method was proposed, but it was not used at experimental data analysis. Finally in Ref. [1] the structure of enhanced graphs and analytical properties of amplitudes were studied. It was shown that the contributions of diagrams corresponding to collective interactions of projectile particles with some of intranuclear nucleons are larger than the contributions of diagrams with binary collisions. This leads to the picture formulated above.

Below in Sec. 2 a simple model of nuclear destruction is formulated that reserves the main ideas of reggeon theory.

We applied the model in Sec.3 for calculation of characteristics of hadron-nucleus and nucleus-nucleus interactions at energies 3.6, 14.6 and 200 *GeV/nucleon*. There we will focus on g-particle distributions in the interactions of ^1H, ^4He, ^{16}O, ^{28}Si and ^{32}S with nuclear photoemulsion. The g-particles are considered very often as direct members of fast stage of the interactions. Their distributions are connected hardly with the nuclear destruction mechanism. As will be shown below, the proposed approach leads to the decreasing of the ejected nucleons multiplicity (comparing with prediction of cascade model) and to satisfactory description of experimental distributions.

The calculations of nucleon contents of residual nuclei (Sec.4), especially the total charge of projectile spectator fragment (Q_{sd}) distributions will be compared with experimental data on light nuclei ^{12}C, ^{16}O, ^{22}Ne and ^{28}Si fragmentation which could not be described by cascade model [6]. Finally, in Sec. 5, we reproduce the dependence of the degree of target-nucleus destruction on the degree of projectile destruction ($< N_g(Q) >$).

2 A model of nuclear destruction in nucleus-nucleus interactions

Schematically, the interaction processes in the impact parameter plane (according to reggeon theory [1]) can be represented as in Fig. 1 on which the positions of projectile hadron is marked by open circle, and the positions of nuclear nucleons by closed circles, points are the coordinates of the reggeon interaction vertices (virtual mesons). As one can see the process has features typical for all branching processes. So for its simulation it seems reasonable to use the corresponding methods.

Fig.1 The branching process in hA–scattering in the impact parameter plane. The positions of the projectile hadron is marked by open circle, the positions of nuclear nucleons by closed circles, and square points are the coordinates of the reggeon interaction vertices

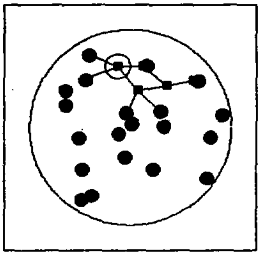

2.1 Model formulation

Let us assume that knock out of a nucleon with impact coordinates $\vec{s}_i$ can initiate the knock out of other nucleon with impact coordinates $\vec{s}_j$ with probability $\phi(|\vec{s}_i - \vec{s}_j|)$. At the same time the second nucleon can initiate a knock out of third one with coordinates $\vec{s}_k$ with probability $\phi(|\vec{s}_j - \vec{s}_k|)$ and so on.

For determination of positions of first ejected nucleons we use Glauber theory, especially DIAGEN code [7]. This permits us to apply the model to the analysis of nucleus-nucleus interactions.

For determination of ϕ, which is needed for Monte Carlo simulation of the processes, let us consider the contribution of simple enhanced diagram of Fig. 2:

Fig.2 Simplest enhanced diagram of hA– interactions. Upper horizontal line presents incident hadron while the lower horizontal lines - the nuclear nucleons. $F_{\pi N}$ is the pion-nucleon scattering amplitude

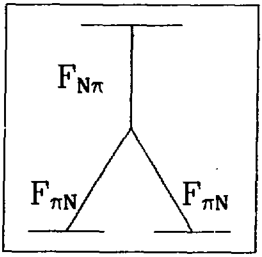

$$
\begin{aligned}
Y &= G\int d\xi' d^2b' F_{N\pi}(\vec{b}-\vec{b}',\xi-\xi') \times \\
&\times F_{\pi N}(\vec{b}'-\vec{s}_1,\xi')F_{\pi N}(\vec{b}'-\vec{s}_2,\xi'), \qquad (1)
\end{aligned}
$$

G is 3-pomeron vertex constant, $\vec{b}$- impact parameter of incident hadron, $\vec{s}_1$, $\vec{s}_2$- impact coordinates of nuclear nucleons. $\vec{b}'$ is the position of pomeron interactions vertex in the impact parameter plane, ξ'-its rapidity.

Using Gaussian parameterization for $F_{\pi N}$ ($F_{\pi N} = exp(-(|\vec{b}|^2)/(R^2_{\pi N}))$ and neglecting its dependence on energy, we have

$$
\begin{aligned}
Y &\simeq G(\xi_0 - 2\epsilon)\frac{R^2_{\pi N}}{3} exp(-(\vec{b}-(\vec{s}_1+\vec{s}_2)/2)^2/3R^2_{\pi N}) \times \\
&\times exp(-(\vec{s}_1-\vec{s}_2)^2/2R^2_{\pi N}), \qquad (2)
\end{aligned}
$$

where $R_{\pi N}$ is the pion-nucleon interaction radius. According to (2) the contribution reaches a maximum if the nucleon coordinates $\vec{s}_1$ and $\vec{s}_2$ coincide and decreases very fast with increasing the distance between the nucleons. For reproduction of this behavior we choose ϕ as

$$
\phi(|\vec{s}_i - \vec{s}_j|) = C exp(-\frac{|\vec{s}_i - \vec{s}_j|^2}{r_c^2}). \qquad (3)
$$

At energies lower than 400 GeV the amplitudes F_{NN} and $F_{\pi N}$ consist of many reggeon contributions. Each of them is characterized by many parameters, $R_{\pi N}$, R_{NN}, g_R,...etc. Thus, we will consider C and r_c only as free parameters.

Furthermore, the expressions under the integrals (e.g. (1)) have not any dependence on nuclear mass A. So it seems natural to assume that ϕ does not depend on A.

2.2 Determination of free parameters

For determination of C and r_c we use the data of Ref. [8] on proton interactions with light (C, N, O) and heavy (Ag, Br) components of emulsion. We assume that the average number of ejected protons $< n_p^{ej} >$ is proportional to the average multiplicity of g-particle. To exclude the proportionality coefficients we shall look for the ratio $R = \frac{<n_p^{ej}>_{Ag,Br}}{<n_p^{ej}>_{C,N,O}}$.

Calculations of ratio R at different values of C and r_c are presented in Fig. 3. As one can see the requested value of the ratio can be reached at different sets of C and r_c. The allowed region of C and r_c is presented by the curve in Fig. 4.

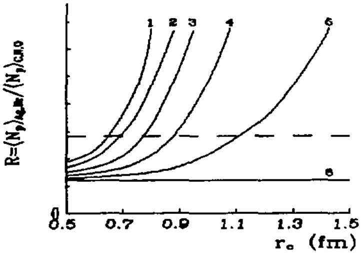

Fig.3 Calculations of ratio R as function of r_c at different values of C, the dashed line represents experimental data of [8] and solid lines of 1 until 5 represents values of C from $C = 1$ to $C = 0.2$ in steps of 0.2. The solid line number 6 represents Glauber limit ($C = 0$)

It is worth mentioning that, calculations of the ejected nucleons multiplicity distributions are not very sensitive to the choice of C and r_c from the allowed region. For concrete calculations $C = 1$ and $r_c = 0.6\ fm$ were used.

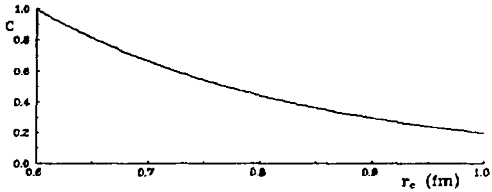

Fig.4 The allowed region of parameters C and r_c where experimental data fall

3 g-particle multiplicity distribution

At experimental studies using photoemulsion the slow charged particles produced in the target fragmentation region are subdivided into b- and g-particles. b-particles have relative velocity $\beta = v/c \leq 0.2$. They are mainly evaporated protons with $T_p \leq 26MeV$ and nuclear residuals. g-particles have velocity $0.2 < \beta < 0.7$ ($26 < T_p < 400MeV$). Mainly they are protons. It is assumed that g-particles are produced at the fast stage of the interaction and directly connected with fast nuclear destruction mechanisms (the slow process of deexcitation of residual nuclei results in b-particles creation).

The average multiplicity of g-particles ($< N_g >$) in hadron-nucleus interactions decreases slightly with energy for given projectile and target, which reflects small variation of collision geometry with increasing energy. At the same time $< N_g >$ increases as $A^{2/3}$ with increasing target mass number. This fact is directly connected with cascading of secondaries. In order to reproduce this behavior in our model, we assume that each ejected proton can be registered as g-particle with probability α. It is determined by energy spectra of protons and low energy threshold of g-particle registrations.

To our knowledge, the shape of proton energy spectra in high energy hadron-nucleus collisions, practically, has not any dependence on target mass number. So, it is natural to assume that α has no A dependence.

Charge exchange reactions like $n \longrightarrow p$ and $p \longrightarrow n$ can influence the value of α. However, taking into account the fact that the number of protons and neutrons in nuclei is nearly equal, we assume that these processes compensate each other.

To consider the geometrical aspects of the collisions we represent a nucleus as a set of nucleons (points) with coordinates distributed according to the densities

$$\rho_A(\vec{r}) = const \quad e^{-\frac{r^2}{r_0^2}}, \quad 4 \leq A \leq 12,$$

$$\rho_A(r) = \frac{const}{(1+e^{(r-R)/c})}, A \geq 12,$$

$$R = 1.07A^{1/3} fm, \quad c = 0.545 fm.$$

To determine the positions of the first ejected nucleons we used code DIAGEN [7]. It requires NN interaction characteristics such as total cross section -σ^{tot}, the slope of differential elastic scattering cross section- B, and the ratio of real to imaginary parts of elastic scattering amplitude at zero momentum transfer-$\delta = \frac{Ref(0)}{Imf(0)}$. The values of used parameters were $\sigma^{tot} = 42mb$, $B = 7.6$ (GeV/c), $\delta = -0.23$ at energies nearly ~ 3.5 $GeV/nucleon$. At high energies ($15 \div 200$ GeV) we used $\sigma^{tot} = 40mb$, $B = 12$ (GeV/c), $\delta = 0$. Cross sections of nucleus interactions with different components of photoemulsion were calculated with the help of DIAGEN.

At reproduction of the ratio of the average multiplicities of g-particles produced in the interactions of protons with light (C, N, O) and heavy (Ag, Br) emulsion nuclei [8], the allowed region of parameters C and r_c was determined (see Sec.2.2). In Ref. [8] the experimental $< N_g >$ is given for the interaction of protons with emulsion at high energy and $< N_p^{cj} >$ is determined by the model at the given values of C and r_c. From this $\alpha = 0.88$.

In Fig. 5 the multiplicity distributions of g-particles for the interactions of protons with emulsion [8] are compared with our calculations. A very good agreement is obtained between experimental data and our model. The same agreement was reached in Ref.[8]. It was assumed there that each intranuclear collision of the incident particle with nuclear nucleons is accompanied by the secondary hadrons interactions in which g-particles creation takes place. The assumption of Ref. [8] is very near to ours (see Sec.2).

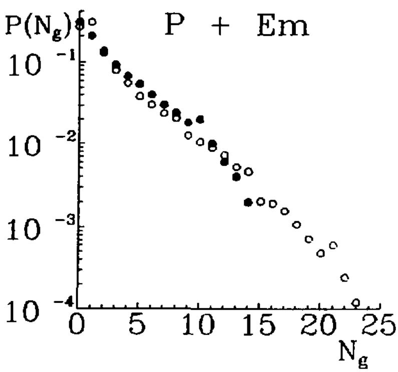

Fig.5 The normalized multiplicity distributions of $g-$particles for the interactions of $P + Em$ [8] (solid points) are compared to our model calculations (open circles)

At description of nucleus-nucleus interactions, the values of our model parameters have not changed at all from that of hadron-nucleus case. Fig. 6 represents the experimental N_g- distributions of ^4He, ^{12}C, ^{16}O, ^{22}Ne and ^{28}Si interactions with photoemulsion at 3.6 $GeV/nucleon$ [9]-[13] as compared with our model. Our calculations decrease more rapidly than experimental data at values of $N_g \geq 15$ in the case of $^4He + Em$. But they reproduce nicely $^{12}C + Em$ data at $N_g \leq 30$. In the case of $^{16}O + Em$, the experimental data is underestimated at $N_g > 26$. This holds also for $^{22}Ne + Em$ and $^{28}Si + Em$ but for values of $N_g > 29$ and 35, respectively. Thus the model can in principle describe the gross features of the data, i.e. N_g- distribution extends to higher N_g values with increasing mass number of the projectile (Cf. Fig. (6)).

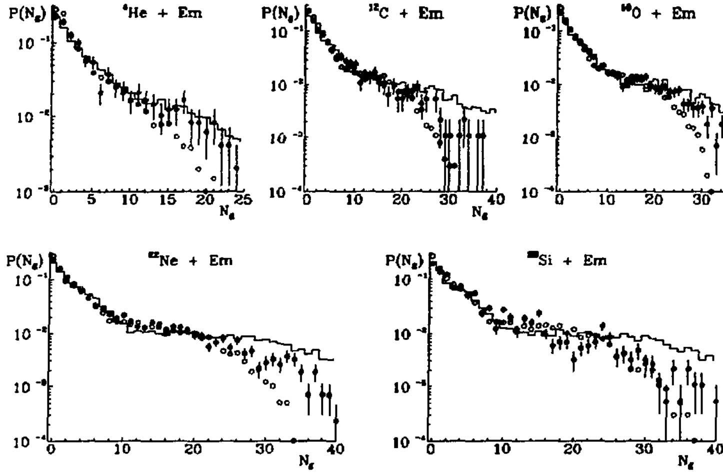

Fig.6 The experimental N_g–distributions of ^4He, ^{12}C, ^{16}O, ^{22}Ne and ^{28}Si interactions with photoemulsion at 3.6 $GeV/nucleon$ (solid points) [9]-[13] are compared to CEM [14] (histograms) and our calculations (open circles)

Cascade evaporation model (CEM) [14], as one can see in Fig. 6, agrees very well with the experimental data of ^4He+Em. However, CEM exceeds the N_g-distribution of ^{12}C and $^{16}O+Em$ at values of $N_g > 20$. In the case of $^{22}Ne + Em$, CEM has a small shift below data in the region $N_g = 2 - 7$ and overestimates the distribution at $N_g > 25$. This is also true in the case of $^{28}Si + Em$. So, one expects that CEM can't describe heavy ion collision data quite correctly.

In Fig. 7, the normalized g-particle multiplicity distributions for the interactions of ^4He, ^{16}O, ^{28}Si, $^{32}S + Em$ at high energies [15] are compared with our model. As can be seen, a very good agreement is obtained without any fitting parameter in different energy ranges.

So our model is successful to fit the data on nucleus-nucleus collisions of *JINR*, *BNL* and *CERN* (with a difference of energy per nucleon of 40) of different projectile masses with no free parameter.

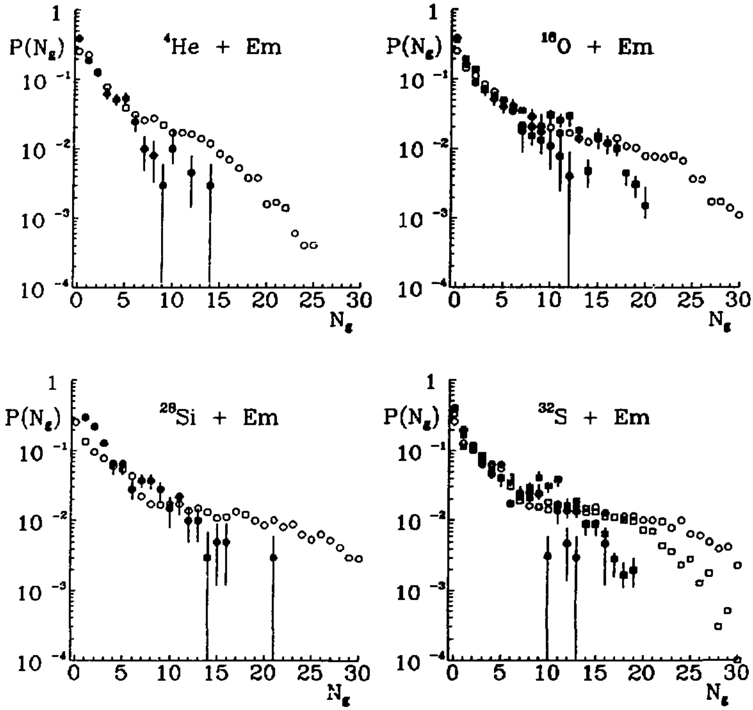

Fig.7 The normalized $g-$particles multiplicity distributions for the interactions of ^4He at 140 $GeV/nucleon$, ^{16}O and ^{32}S at 200 $GeV/nucleon$, ^{28}Si at 14.6 $GeV/nucleon$ (solid points) [15] are compared to our model (open circles). In the case of ^{16}O and ^{32}S two data samples are presented (closed circles [15] and squared points [18]). Also, we represent our calculations with $C = 0.8$ (open squares) in the case of $S + Em$

4 Q_{zd}–distributions and other characteristics

In order to examine the validity of our model in the projectile region we discuss so called Q_{zd}–distribution. The quantity Q_{zd} measures the charge flow observed in a narrow forward cone $\theta < 0.6/p_{beam}$ of the projectile remnant (p_{beam} is the beam momentum per nucleon). In Fig. 8, the experimental Q_{zd} multiplicity distributions for interactions of ^{12}C, ^{22}Ne and $^{28}Si + Em$ at 3.6 $GeV/nucleon$ are compared to our model. We determined Q_{zd} as $Z - N_p$, where Z is the charge of projectile nucleus and N_p is the total number of ejected protons. As one can see a good description is obtained.

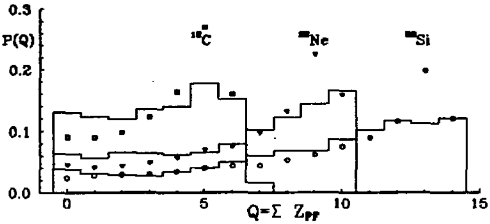

Fig.8 The experimental Q_{zd}-distributions for interactions of ^{12}C, ^{22}Ne and $^{28}Si + Em$ at 3.6 $GeV/nucleon$ [9]-[13] are compared to our model calculations (points)

The data sample of ^{12}C shows a rise at smaller Q_{zd} values, which might signal a somewhat larger stopping power, i.e. it is harder for this projectile nucleus to penetrate the target nucleus than predicted by the model. However, in the case of ^{22}Ne and $^{28}Si + Em$, their destruction can be described by our model. On the other hand, cascade model cannot give good results [6].

At CERN experimental studies of nucleus-nucleus interactions the zero-degree calorimeter (ZDC) was used to determine the energy entering the forward direction with $\theta < 0.3$ [16]. The energy (E_{zdc}) is a good measure of the nuclear stopping power. Also, we think that E_{zdc}–distributions reflect the residual nucleus mass number distributions. The last ones depend only on C and r_c in our model. Here, also, we have not additional parameters but we reproduce quite well E_{zdc}–distributions. In Fig. 9, the experimental E_{zdc}–distributions for interactions of $^{16}O + ^{12}C$, ^{64}Cu, ^{108}Ag and ^{197}Au at 60 $GeV/nucleon$ with calculations of FRITIOF [16] and our model are given. We determined E_{zdc} as a product of 60 GeV and the number of spectator nucleons. We did not take into account experimental conditions. As one can see the agreement between data and our model calculations is satisfactory.

In the $^{16}O + ^{197}Au$ interaction, there is a pronounced peak at the lowest energies. These events with low ZDC energies result from collisions in which the oxygen projectile is engulfed by the massive Au nucleus, resulting in the emission of only a few leading particles at angles less than 0.3°. Furthermore, in this case, a wide range of impact parameters gives rise to collisions in which the entire projectile interacts with a nearly constant number of target nucleons, thus producing the peak at low ZDC energies. For $O + C$ interactions the wide range of impact parameters is very small so there is no peak at low E_{zdc}. These behaviors can be reproduced by our model.

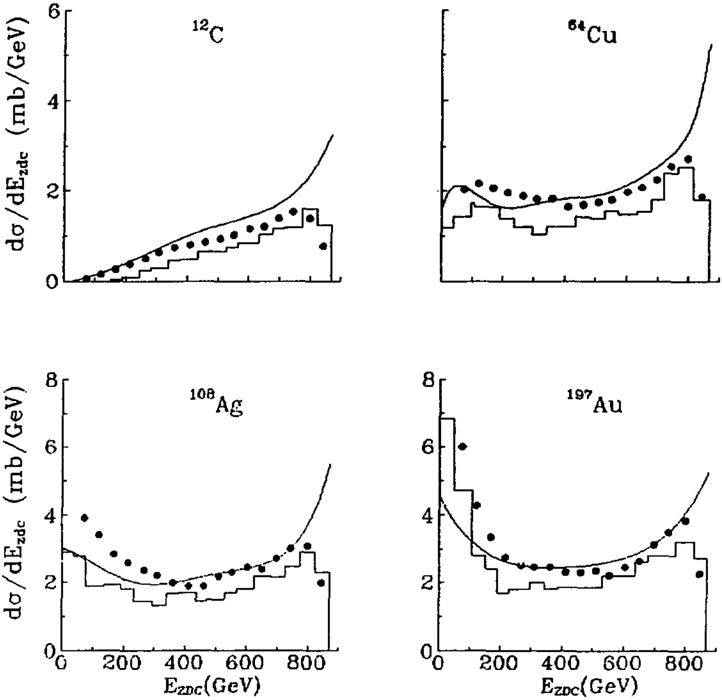

Fig.9 The experimental E_{zd}–distributions for interactions of $^{16}O +^{12} C$, ^{64}Cu, ^{108}Ag and ^{197}Au at 60 *GeV/nucleon* are compared with calculations of FRITIOF [16] (histogram) and our model (solid lines)

There is discrepancy between our model calculations and experimental data at large values of E_{zdc}. This is because we do not include in our calculations the minimum- bias condition [16]. This condition is defined by the requirements that

- less than 88% of the full projectile energy is measured by the ZDC,
- at least one charged particle is recorded by the multiplicity arrays in the interval $1.3 < \eta < 4.4$.

So, peripheral events with low multiplicity of produced particles were omitted. The percentage of these events decreases with increasing target mass number and a good description in this region for $^{16}O + ^{108}Ag$, ^{197}Au interactions is obtained.

5 Correlation between projectile and target nucleus destructions

Consider now the correlation between the mean number of g-particles $< N_g >$ as function of Q_{zd}. It was shown [17, 18] in an analysis of ^{16}O interactions with emulsion that $< N_g >$ for interactions at 14.6, 60 and 200 $GeV/nucleon$ scale as a function of Q_{zd}. According to our model, this scaling is obvious, because our parameters C, r_c and α have no energy dependence. More interesting is the dependence $< N_g(Q_{zd}) >$ on A. Fig. 10 shows the experimental data of $< N_g >$ as function of Q_{zd} for interactions of O and S with emulsion at 200 $GeV/nucleon$ [17, 18]. As can be seen, the mean value of N_g increases almost linearly with decreasing values of Q_{zd} (i.e. increasing centrality of the collision). We have a good agreement, with no free parameter, for $^{16}O + Em$ collisions. However, in the case of $^{32}S + Em$ our calculations overestimate experimental data at low values of Q_{zd}.

There can be at least two reasons for discrepancy:

- the difference between experimental methods used by authors of papers[17, 18],
- it is a defect of the model.

Two existing sets of ^{16}O-data [17. 18] are different for small values of Q_{zd} (see Fig. 10). This can be due to different experimental conditions or to low statistics. At the moment we cannot choose from the last two possibilities. The more exact data are needed. We hope if the agreement between experimental data is reached, it will reflect on S data.

At JINR energies our model somewhat underestimates the tails of g−particle multiplicity distributions for ^{16}O and ^{22}Ne interactions with emulsion (see Fig. 6). However at CERN data we have a tendency to overestimate slightly the tails of the distributions (see Fig. 7). This means that the effective constants C, r_c or α have weak energy dependence. The change of α can be checked at experimental studies of proton momentum distributions in high energy nucleus-nucleus collisions. To estimate C and r_c more exactly we need to perform complete theoretical considerations. The easiest way now is to change C to obtain an agreement with data. In Fig. 10 the calculations with $C = 0.8$ are presented (see also Fig. 7). As one can see this permits somewhat better description of $^{32}S + Em$ data but breaks the agreement with $^{16}O + Em$ data. So the agreement cannot be reached by simple change of model parameters.

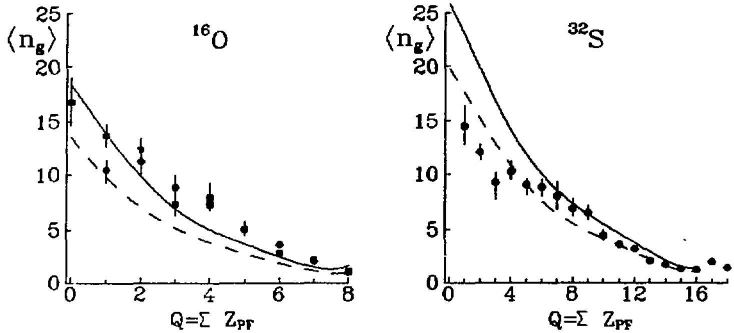

Fig.10 The experimental data of $< N_g >$ as function of Q_{zd} for interactions of ^{16}O (two data samples [17, 18] are presented by squares and circles, respectively) and ^{32}S with emulsion at 200 $GeV/nucleon$ are compared to our calculations with $C = 1$ (solid lines) and $C = 0.8$ (dashed lines)

6 SUMMARY

The reggeon theory assumes that cascading is a collective phenomenon contrary to the familiar cascade models, which consider an interaction as a set of binary nucleon-nucleon and meson-nucleon collisions. This means that at small impact parameters no separate nucleons are ejected from the nucleus but a group of them with closed impact parameters. Inspired by this approach, a nuclear destruction model is presented. In the framework of the model we **satisfactorily described the following:**

- g-particles multiplicity distribution in nucleus-nucleus interactions at 3.6 $GeV/nucleon$. The agreement is reached even to higher N_g−values than CEM;
- At 14.6 and 200 $GeV/nucleon$, the g-particles multiplicity distributions in nucleus-nucleus interactions. A good agreement is also obtained without any free parameters;
- Q_{zd}− and E_{zdc}−distributions;
- The mean number of g−particles as a function of Q_{zd} for O, $S + Em$ at 200 $GeV/nucleon$.

All of these show us that reggeon theory can be a good competitor to the familiar cascade models and can be applied at high and superhigh energies.

References

[1] K. G. Boreskov, A. B. Kaidalov, S. T. Kiselev, N. Ya. Smorodinskaya, Yad. Fiz, **53**, 569 (1991) (Sov. J. Nucl Phys. **53** (1990)).

[2] R. Jengo, D. Treliani, Nucl. Phys. **117B**, 433 (1976).

[3] R. E. Gamboa Saravi, Phys. Rev. D **21**, 2021 (1980).

[4] A. Schwimmer, Nucl. Phys. **94B**, 445 (1975).

[5] L. Caneschi, A. Schwimmer, R. Jenco, Nucl. Phys. **108B**, 82 (1976).

[6] A. El-Naghy et al., J. Phys. G **14**, 1125 (1988).

[7] S. Yu. Shmakov, V. V. Uzhinskii, A. M. Zadorozhny, Com. Phys. Comm. **54**, 125 (1989).

[8] E. Stenlund, I. Otterlund, Nucl. Phys. **198B**, 407 (1982).

[9] E. S. Basova et al., Z. Phys. A **287**, 393 (1978).

[10] A. Marin et al., Yad. Fiz. **29**, 105 (1979) (Sov. J. Nucl Phys. **29** (1979)).

[11] V. A. Antonchik et al., Yad. Fiz. **39**, 1228 (1984) (Sov. J. Nucl Phys. **39** (1984)).

[12] N. P. Andreeva et al., Yad. Fiz. **45**, 123 (1987) (Sov. J. Nucl Phys. **45** (1987)).

[13] N. P. Andreeva et al., Yad. Fiz. **45**, 1010 (1987) (Sov. J. Nucl Phys. **45** (1987)).

[14] V. S. Barashenkov, F. Zh. Zheregy, Zh. Zh. Musulmanbekov, preprint JINR, P2 - 83 -117, Dubna, 1983, unpublished.

[15] P. L. Jain, G. Singh, and K. Sengupta, Phys. Rev. C **43**, R2027 (1991); P. L. Jain et al., Phys. Rev. C **44**, 844 (1991).

[16] S. P. Sorensen et al., Z. Phys. C **38**, 3 (1989).

[17] M. I. Adamovich et al., Phys. Lett. **262B**, 369 (1991).

[18] A.Dubrowska et al. (KLM collaboration), Phys. Rev. D **47**, 1751 (1993).

Received by Publishing Department
on April, 11, 1994.